

Exactly Soluble Addition and Condensation Models in Coagulation Kinetics

E. M. HENDRIKS AND M. H. ERNST

Institute for Theoretical Physics, Princetonplein 5, P.O. Box 80.006, 3508 TA Utrecht, The Netherlands

Received January 17, 1983; accepted June 6, 1983

The kinetics of clustering through addition ($a_k + a_1 \rightarrow a_{k+1}$) and condensation ($a_j + a_k \rightarrow a_{j+k}$, $j \neq 1, k \neq 1$) for a model of cylindrically shaped monomeric units a_1 are studied, using Smoluchowski's coagulation equation, and analytic solutions for several limiting cases (flat disks and needles) with and without condensation reactions, were given. The condensation models of flat disks and needles include, respectively, the linear polymer model RA_2 and the branched polymer model A_2RB_∞ (with a gelation transition). If condensation reactions are inhibited, we obtain exactly soluble addition models with a monomer-cluster rate constant independent of or proportional to the cluster size. The monomers are (i) supplied in a given amount at the initial time; (ii) generated by a steady source; or (iii) supplied by an infinite reservoir that keeps the concentration of monomers, $c_1(t)$, constant in time.

1. INTRODUCTION

In this paper we discuss models for clustering or coagulation processes, resulting from addition and condensation reactions, occurring in many fields of science; e.g., atmospheric physics (1), polymer science (2), colloid chemistry (3), hematology (4), etc. The clustering process is initiated by a primary source of fine grained particles or monomeric units a_1 .

In the *early stages of clustering* the basic mechanism of growth proceeds via fine grained particles, that can either stick to larger particles or to each other, according to the addition reaction $a_k + a_1 \rightarrow a_{k+1}$.

This reaction scheme enters in a variety of clustering problems, such as birth and death processes (5), aerosol agglomeration in gas to particles conversion systems (6–10), polymerization (11), flocculation (3), aggregation of red blood cells (4).

In the *next stage of the growth process*, when the amount of monomers becomes depleted or the concentrations of monomers and of k -mers become comparable, *condensation reactions* ($a_j + a_k \rightarrow a_{j+k}$; $j, k > 1$) become important (12–15). The time evolution of the

size distribution or concentration $c_k(t)$ of k -mers is then given by Smoluchowski's coagulation equation (1):

$$dc_k/dt = \frac{1}{2} \sum_{i+j=k} K_{ij}c_i c_j - c_k \sum_{j=1}^{\infty} K_{kj}c_j, \quad [1.1]$$

to be solved subject to the monomer initial condition $c_k(0) = M\delta_{k1}$ (where M is the concentration of monomers initially put into the system). K_{ij} is the bimolecular rate constant for coagulation of an i -mer and a j -mer, and fragmentation reactions have been neglected in [1.1]. A fundamental property of [1.1] is the conservation of total mass $\sum kc_k(t) = M$. Certain condensation reactions, however, lead to a violation of mass conservation after a finite time, which is interpreted as being caused by the appearance of an infinite cluster or gel (13, 14). This phenomenon, to which we will briefly return in Section 2, is called gelation in polymer science.

Also growth processes by condensation reactions form a *transient stage* in the process of clustering. As clusters are growing in size, *break up processes become important* and the clustering process should be described by the

reversible reaction $a_i + a_k \rightleftharpoons a_{i+k}$. The rate equations read then (2):

$$\dot{c}_k = \frac{1}{2} \sum_{i+j=k} [K_{ij}c_i c_j - F_{ij}c_{i+j}] - \sum_{j=1}^{\infty} [K_{kj}c_k c_j - F_{kj}c_{k+j}], \quad [1.2]$$

where F_{ij} is the rate constant of the reverse (fragmentation) reaction and K_{ij} that for the forward (coagulation) reaction. By Arrhenius' law (15) F_{ij}/K_{ij} is proportional to $\lambda = \exp(g/k_B T)$, where g is the binding energy of a single bond ($g < 0$), T is the temperature and k_B is Boltzmann's constant. Only for very strong bonds ($g \rightarrow -\infty$) fragmentation may be neglected, and the rate equations [1.2] reduce to the coagulation Eq. [1.1].

The kinetic equations for reversible coagulation (2, 16–20) yield more realistic size distributions for large times; e.g., the “most probable solutions” in the Flory–Stockmayer theory of polymerization (12, 21) for a given extent of reaction can be found as the stationary solution of the kinetic equations of reversible polymerization (20).

Of course, many more limitations are inherent to the coagulation equation for modeling the kinetics of clustering (22). Nevertheless, it is of interest to idealize certain coagulation processes as irreversible additions or condensation reactions, and construct extremely simplified, but exactly soluble models from which certain details such as asymptotic properties of the time dependence of the size distribution and its moments can be obtained. The actual values of the physical parameters determine to what extent (time interval, cluster size) the above models are relevant for the coagulation process under consideration. In addition, these models may be used to test numerical methods for solving the infinite set of coupled nonlinear rate equations with more realistic clustering mechanisms.

In this philosophy we start from a coagulation model (SP-model), introduced by Sam-

sel and Perelson (4) to describe the aggregation of red blood cells (rouleaux formation) with some minor modifications. Samsel and Perelson have performed extensive numerical studies of coagulation kinetics in the above model at different values of the physical rate constants. Our exactly soluble models may be considered as special limiting cases of this model.

In Section 2 we will discuss condensation models and in the remaining sections, addition models with initial monomer supply (Section 3), with a steady source (Section 4), and with an infinite reservoir (Section 5).

2. ADDITION AND CONDENSATION MODELS

Flat Disk Model (Condensation Model A)

In this section we give a short description of the SF-model, from which the flat disk and needle model can be obtained as limiting cases. The coagulation equations for these condensation models are given, and some analytic results for the monomer and the total cluster concentration are derived. A special case of the needle model corresponds to Flory's polymer model A_2RB_∞ (21) for which the analytic solution for size distribution and moments are given explicitly both for irreversible and reversible coagulation reactions. Next, we idealize cases of condensation reactions with very small rate constants as pure addition reactions, and present the kinetic equations for the resulting addition models.

The SF-model describes the coagulation kinetics of cylindrically shaped units (monomers): its caps are uniformly covered with reactive A-groups (surface area s) and its walls (surface area w) with reactive B-groups. One allows cap–cap reactions (A–A bonds) leading to elongation of linear chain segments, and cap–wall reactions (A–B bonds) leading to branching.

Here we only consider two limiting cases. If $w \ll s$, the monomers are flat disks, the basic coagulation mechanism is through cap–cap reactions, and the majority of clusters consist

of linear chains with A-A bonds.¹ We, therefore, consider the limiting case, $w = 0$, in which each cluster has two caps (no branching). If the mobility of the clusters is sufficiently large, such that the reaction rates are not limited by diffusion, then the coagulation coefficient is proportional to the number of ways in which two clusters can be connected. In the present case there are three possibilities independent of the sizes of the reacting clusters, so that K_{ij} is a constant:

$$K_{11} = \epsilon, K_{1j} = 1, \\ K_{ij} = \gamma \quad (i \neq 1, j \neq 1). \quad [2.1]$$

The parameters (ϵ, γ) may be used to account for differences in rate constants between monomers and clusters (dimers, trimers, . . .) e.g., there may be mechanisms lowering the reactivity of functional groups on clusters, or one may model the smaller mobility of clusters compared to that of monomers, by smaller γ -values ($\gamma < \epsilon, 1$). The Smoluchowski equation for the flat disk model reads then:

$$dc_1/dt = -\epsilon c_1^2 - c_1 R \\ dc_2/dt = 1/2 \epsilon c_1^2 - c_1 c_2 - \gamma c_2 R \\ dc_k/dt = c_1 [c_{k-1} - c_k] \\ + 1/2 \gamma \sum_{i+j=k} c_i c_j - \gamma c_k R, \quad [2.2]$$

where $i, j, k > 2$ and R represents the number of clusters, defined as

$$R(t) = \sum_{k=2}^{\infty} c_k(t). \quad [2.3]$$

Mass conservation, $\sum_{k=1}^{\infty} k c_k(t) = M$, is valid for all times, and no gelation transition occurs, as $\sum k^2 c_k(t)$ remains bounded on bounded time intervals (23). In the special case, $\epsilon = \gamma = 1$, the model reduces to a standard growth model for linear polymers, where the analytic

solution of [2.2] is well-known (1). Samsel and Perelson have made extensive numerical studies of [2.2] for different values of (ϵ, γ) .

For general (ϵ, γ) we have obtained analytic solutions for the concentration of monomers, $c_1(t)$, and for the total concentration of clusters, which satisfies

$$dR/dt = 1/2 \epsilon c_1^2 - 1/2 \gamma R^2. \quad [2.4]$$

This equation can be derived by summing the equations for $c_k(t)$ in [2.2]. Dividing [2.4] by the equation for c_1 enables us to eliminate the t variable and to consider $R(t)$ as a function of $c_1(t)$. Introduction of the variables $x = c_1$ and $y = R/c_1$ yields the differential equation:

$$x dy/dx \\ = [(\gamma - 2)y^2 - 2\epsilon y - \epsilon]/(2\epsilon + 2y). \quad [2.5]$$

Since $c_1(0) = M = 1$ and $R(0) = 0$,² this equation should be solved subject to the boundary condition $y = 0$ and $x = 1$. The solution, found by standard methods, can be written as

$$x^{(\gamma-2)(y_1-y_2)/2} \\ = (1 - y/y_1)^{\epsilon+y_1} (1 - y/y_2)^{-\epsilon-y_2} \quad [2.6]$$

with the following definitions:

$$y_{1,2} = \delta \pm (\delta^2 + \delta)^{1/2}, \quad \delta = \epsilon/(\gamma - 2). \quad [2.7]$$

This result enables one to plot R as a function of c_1 ($0 < c_1 < 1$), as we have done in Fig. 1 for the rate constants $K_{11} = \epsilon$ and $K_{ij} = \gamma$ ($i, j > 1$).

The time dependence of $c_1 = x$ and $R = xy$ can be obtained by quadrature, using [2.4], [2.5], and [2.6] and yields

$$t = [2/(2 - \gamma)] \\ \times \int_0^y dy [x(y')(y' - y_1)(y' - y_2)]^{-1}. \quad [2.8]$$

² If one denotes concentrations of monomers and clusters for the case $M \neq 1$ respectively as $c_1(t; M)$ and $R(t; M)$, one easily verifies that $c_1(t; M) = M c_1(Mt; 1)$ and $R(t; M) = M R(Mt; 1)$.

¹ In the SF-model for aggregation of red blood cells the cap diameter is about 3 times as large as the height of the disk.

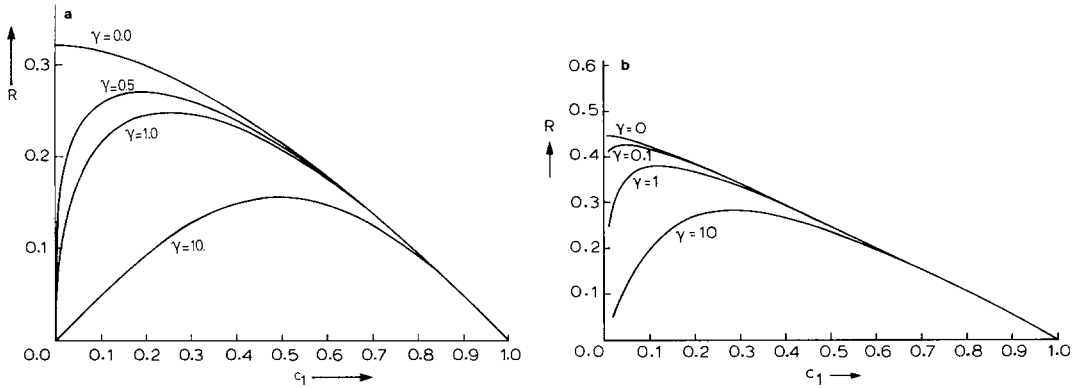


FIG. 1. Cluster concentration $R = \sum_{k=2}^{\infty} c_k$ versus monomer concentration c_1 in condensation model A ($c_1 \rightarrow 0$ corresponds to $t \rightarrow \infty$) for different condensation rate constants $K_{ij} = \gamma$ ($i, j > 1$) ($\gamma = 0$ yields addition model A) with a monomer–monomer rate constant (a) $K_{11} = 1$ and (b) $K_{11} = 10$.

By numerically performing this integral we have obtained graphs of $c_1(t)$ and $R(t)$ for different values of the rate constant $K_{ij} = \gamma$ ($i, j > 1$) and $K_{11} = \epsilon$, as shown in Fig. 2.

In some special cases the expressions simplify. For instance for $\gamma = 2$ we have instead of [2.6] and [2.8]:

$$x = (1 + 2y)^{-1+(1/2\epsilon)} \exp(-y/\epsilon)$$

$$t = \epsilon^{-1} \int_1^{1+2y} dz z^{-(1/2\epsilon)} \exp\{(z-1)/2\epsilon\}. \quad [2.9]$$

For long times, when the concentration of monomers becomes vanishingly small, [2.6] predicts for $\gamma > 2$ that $y \uparrow y_1$ or $R \simeq y_1 c_1$. For $\gamma = 2$ one finds from [2.9] $R \simeq -\epsilon c_1 \ln c_1$ ($c_1 \rightarrow 0$) and for $\gamma < 2$, from [2.6] $R \simeq A c_1^{\gamma/2}$ where A can be easily calculated. This last result contains the simple case $\epsilon = \gamma = 1$, where the relation $R = \sqrt{c_1 - c_1}$ holds for all times. These results can be understood as follows. When γ is large ($\gamma > 2$), the condensation reactions proceed fast, such that for long times the total number of clusters R decreases proportional to c_1 . For $\gamma < 2$ the condensation reactions are slowed down so that $R \sim (c_1)^{\gamma/2}$ decreases slower than c_1 as $c_1 \rightarrow 0$.

If condensation reactions are much slower than addition reactions (i.e., when $\gamma \ll 1$), condensation may be neglected in [2.2] for a

long period of time, determined by the relation $c_1 > \gamma R$. The rate equations for the addition reaction, obtained by putting $\gamma = 0$ will be discussed at the end of this section. They have been studied numerically by Samsel and Perelson.

Needle Model

If the wall area of a cylindrical monomer is much larger than its cap area, i.e., $w \gg s$, the monomers are needle-shaped, the basic coagulation mechanism is through cap-wall reactions where each A–B bond gives rise to a new branch. The majority of clusters have only A–B bonds and are highly branched. We therefore consider the limit, $s = 0$, with a single reactive A-group on each cap. As each additional unit in a k -mer adds an extra cap, a k -mer has $(k + 1)$ A-groups. The number of B-groups on a k -mer is proportional to its wall-surface, which in turn is proportional to k . Therefore, the number of possible A–B bonds between an i -mer and a j -mer is proportional to $[(i + 1)j + (j + 1)i]$. This yields the corresponding coagulation coefficient:

$$K_{ij} = (2ij + i + j) \begin{cases} \epsilon & \text{if } i = j = 1 \\ 1 & \text{if } i = 1, j \neq 1 \\ \gamma & \text{if } i \neq 1, j \neq 1 \end{cases} \quad [2.10]$$

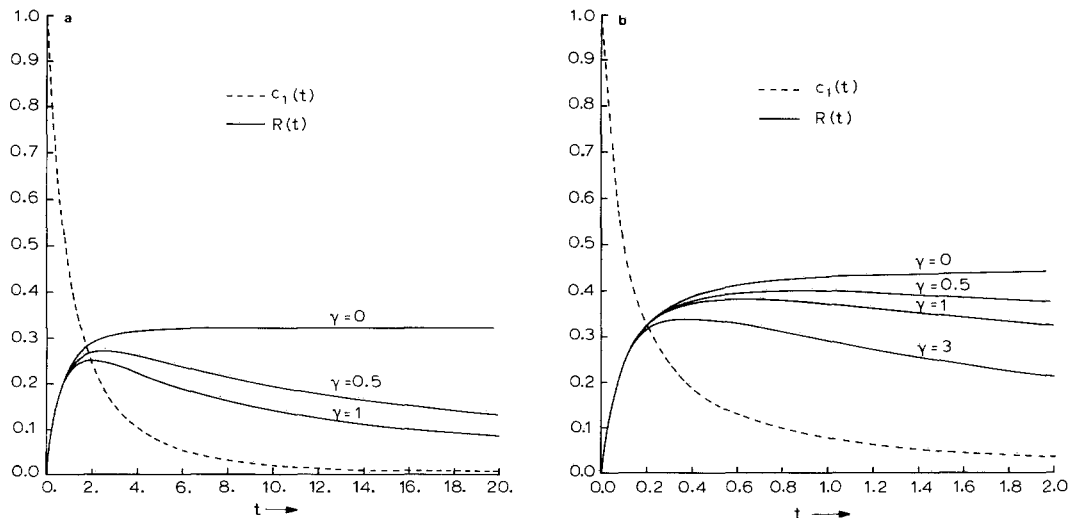


FIG. 2. Monomer concentration $c_1(t)$ and total cluster concentration $R(t)$ versus time in condensation model A for different condensation rate constants $K_{ij} = \gamma$ ($i, j > 1$) ($\gamma = 0$ yields addition model A) with (a) $K_{11} = 1$ and (b) $K_{11} = 10$ as monomer-monomer rate constant. The curves for $c_1(t)$ (drawn as a single curve) depend only weakly on γ . For $t < 6$ they are indistinguishable on the present scale and for $t > 6$ the difference between the curves for $\gamma = 0$ and $\gamma = 1$ is always smaller than 0.02.

The parameters (ϵ, γ) account for differences in the rate constants for reactions between monomers and clusters. This model exhibits a gelation transition. Hence, beyond the gel point³ t_c the sol mass is no longer conserved. For general values of the parameters (ϵ, γ) we have not been able to determine the size distribution $c_k(t)$ or the macroscopic variables $c_1(t)$ and $R(t)$. However, for the simple case $\epsilon = \gamma = 1$, the coagulation coefficients [2.10] correspond to Flory's (21) polymer model A_2RB_∞ (monomers with 2 A-groups, f B-groups ($f \rightarrow \infty$), clusters are branched, have only A-B bonds and no cycles).

The size distribution and moments for the irreversible and reversible condensation model with a general bilinear kernel $K_{ij} = A + B(i + j) + Cij$ and with $c_k(0) = \delta_{k1}$ have recently been determined by Van Dongen and Ernst (20). If their results are applied to the A_2RB_∞ model with $K_{ij} = 2ij + i + j$ and $F_{ij} = 0$ the

size distribution becomes in the *pre-gelation stage* ($t < t_c = \frac{1}{2} \ln 2$ or $\alpha(t) < \alpha_c = 1 - 1/\sqrt{2}$):

$$c_k(t) = N_k \alpha^{k-1} (1 - \alpha)^{k+1} e^{-2\alpha k}, \quad [2.11a]$$

where the extent of reaction α is

$$\alpha(t) = 1 - e^{-t}, \quad [2.11b]$$

and the N_k are determined from the recursion relation:

$$(k - 1)N_k = \frac{1}{2} \sum_{i+j=k} K_{ij} N_i N_j \quad (N_1 = 1). \quad [2.12]$$

For large k these numbers behave as:

$$N_k \simeq [2\pi(2 + \sqrt{2})]^{-1/2} \times k^{-5/2} \xi_c^{-k} \quad (k \rightarrow \infty) \quad [2.13a]$$

with

$$\xi_c = \frac{1}{2}(\sqrt{2} - 1) \exp[\sqrt{2} - 2], \quad [2.13b]$$

and the moments are given by

$$\begin{aligned} M_0(t) &= 1 - 2\alpha, \\ M_1(t) &= 1 \\ M_2(t) &= 1/(1 - 4\alpha + 2\alpha^2). \end{aligned} \quad [2.14]$$

³ We have not determined the value of t_c , where $\sum k^2 c_k(t_c)$ diverges, but the following bounds can be easily established: $\frac{1}{2} M_0^{-1} \ln 2 < t_c < \frac{1}{2} m_0^{-1} \ln 2$, where $m_0 = \min(\epsilon, \gamma, 1)$ and $M_0 = \max(\epsilon, \gamma, 1)$.

In the *post-gelation stage* ($t \geq t_c$) we have the following result for $Q(t) = \{c_k(t), M_0(t), M_1(t)\}$:

$$Q(t) = Q(t_c)/g(t) \quad [2.15a]$$

with

$$g(t) = 1 + b(t - t_c), \quad [2.15b]$$

and

$$b = 2 + \sqrt{2}; \quad c_k(t_c) = (\sqrt{2} + 1)N_k \xi_c^k \\ M_0(t_c) = \sqrt{2} - 1; \quad M_1(t_c) = 1, \quad [2.16]$$

whereas $M_n(t_c) = \infty$ for $n \geq 2$.

For *reversible coagulation* the A_2RB_∞ model (with $F_{ij} = \lambda N_i N_j K_{ij} / N_{i+j}$ and $K_{ij} = 2ij + i + j$ yields according to the method of (20) in the *pre-gelation stage* ($\alpha(t) < \alpha_c = 1 - 1/\sqrt{2}$) the results [2.11]–[2.14], where the extent of reaction in [2.11b] is now given by

$$\alpha(t) = (1 + \lambda)^{-1} \{1 - \exp[(1 + \lambda)t]\} \quad [2.17]$$

with $\lambda = \exp(g/k_B T)$, as defined below [1.2]. For $\lambda > \lambda_0$ (here $\lambda_0 = 1 + \sqrt{2}$), i.e., for small binding energies, one sees that $\alpha(\infty) < \alpha_c$. Hence, the gelation transition is suppressed for sufficiently weak bonds. For $\lambda < \lambda_0$ gelation occurs at the gel-point t_c , determined by the condition $\alpha(t_c) = \alpha_c$. The post-gelation solutions ($t > t_c$) are again given by [2.15] and [2.16] with $g(t)$ in [2.15b] replaced by

$$g(t) = \lambda^{-1} \{ \lambda_0 + (\lambda - \lambda_0) \\ \times \exp[-\sqrt{2}\lambda(t - t_c)] \}. \quad [2.18]$$

If $\gamma \ll 1$ the condensation reactions may be neglected during the period in which the loss of k -clusters through addition reactions is much larger than the loss through the condensation reactions. The rate equations for the resulting model (putting $\gamma = 0$) read

$$dc_1/dt = -4\epsilon c_1^2 - c_1 \sum_{j=2}^{\infty} s_j c_j \\ dc_2/dt = 2\epsilon c_1^2 - s_2 c_1 c_2 \\ dc_k/dt = c_1 [s_{k-1} c_{k-1} - s_k c_k], \quad [2.19]$$

where the rate constant for monomer-cluster reactions, $K_{1k} = s_k \equiv 3k + 1$, ($k \geq 2$) is for large k proportional to the size of the cluster. A closely related addition model with $s_k = k$

will be discussed in the next subsection. We did not succeed in solving the addition model with $s_k = 3k + 1$, but we expect that the model with $s_k = 3k$ yields essentially the same results for the size distribution, except for the smallest cluster sizes.

Condensation model B. For later comparison with the addition model with $s_k = k$ ($k \geq 2$) we briefly consider the condensation model:

$$K_{11} = \epsilon, \quad K_{1j} = j, \\ K_{ij} = \gamma ij \quad (i \neq 1, j \neq 1), \quad [2.20]$$

which exhibits a gelation transition. The simple case, $\epsilon = \gamma = 1$, corresponds to the polymer model RA_∞ (monomers with f A-groups ($f \rightarrow \infty$); A–A bonds; branched polymers without cycles). In the *pre-gelation stage* ($t < t_c = 1$ or $\alpha(t) < \alpha_c = 1$) the size distribution and moments are (13, 14):

$$c_k(t) = N_k \alpha^{k-1} e^{-\alpha k} \\ M_0(t) = 1 - 1/2\alpha; \quad M_1(t) = 1; \quad M_2 = (1 - \alpha)^{-1} \\ R(t) = M_0(t) - c_1(t) = 1 - 1/2\alpha - e^{-\alpha} \quad [2.21]$$

with $\alpha(t) = t$ and $N_k = k^{k-2}/k!$. In the *post-gelation stage* we have for $Q = \{c_k, M_0, M_1\}$ the result:

$$Q(t) = Q(t_c)/g(t) \quad [2.22]$$

with $g(t) = t$. All moments $M_n(t) = \infty$ for $n \geq 2$ and $t \geq t_c$.

For *reversible coagulation* the RA_∞ model yields according to the method of (20) in the *pre-gelation stage* ($\alpha(t) < \alpha_c = 1$) the results [2.21] with α replaced by $\alpha(t) = (1 - e^{-\lambda t})/\lambda$. For $\lambda > \lambda_0 = 1$ (weak bonds) the gelation transition is suppressed. For $\lambda < \lambda_0 = 1$ gelation occurs at the gel point $t_c = -\lambda^{-1} \times \ln(1 - \lambda)$. The post-gelation solutions are given by [2.22] with $g(t) = (1 - e^{-\lambda t})/\lambda$.

For general values of the parameters (ϵ, γ) we have the *pre-gelation* results:

$$c_1(t) = \{1 - \epsilon + \epsilon e^t\}^{-1} \\ R(t) = 1/2(1 - \epsilon)^{-1}(\epsilon - \gamma)[c_1(t) - 1] \\ + 1/2(1 - \epsilon)^{-2}(\gamma + \epsilon - 2\epsilon\gamma) \ln c_1(t) \\ + 1/2(1 - \epsilon)^{-2}\epsilon(1 - \epsilon\gamma)t. \quad [2.23]$$

In Fig. 3 we have plotted $R(t)$ for the case $\epsilon = 1$ and various choices of γ . The graphs are valid up to the gel point t_c , defined through the relation $M_2(t_c) = \infty$, and determined numerically from the second moment equation. The post-gelation result is only known for $\epsilon = \gamma = 1$ through [2.22].

Addition Models

The addition models to be discussed are limiting cases of coagulation models, in which the cluster-cluster reactions have very small rate constants ($\gamma \ll 1$). Putting $\gamma = 0$, we obtain the rate equations for addition reactions. The coagulation coefficients then have the general form $K_{ij} = s_i \delta_{j1} + s_j \delta_{i1}$, where $K_{11} = 2s_1$ is the rate constant for monomer-monomer reactions and $K_{1k} = s_k (k \geq 2)$ that for monomer-cluster reactions. The kinetic equations attain the simple form:

$$dc_1/dt = -s_1 c_1^2 - c_1 \sum_{j=1}^{\infty} s_j c_j + Q$$

$$dc_k/dt = c_1 (s_{k-1} c_{k-1} - s_k c_k) \quad (k \geq 2), \quad [2.24]$$

where we have added a (possibly vanishing) source term Q , representing the rate of monomer production by an external source. The total mass balance is therefore given by $\sum k dc_k/dt = Q$. If the concentration $c_1(t)$ of monomers does not significantly change with time, $c_1(t)$ may be approximated by a constant and the rate equations become linear. This approximation is exact if the system is coupled to a reservoir that emits monomers. In general, however, the monomers are given at the initial time in a total amount M or produced at a given rate Q , and the rate equations are non-linear. We will investigate how these different circumstances affect the addition process.

The rate constants $K_{1k} = s_k (k \geq 2)$ in our addition models are either independent of the cluster size ($s_k = S$) or proportional to it ($s_k = Sk$), where S is some constant. The monomers are supplied in one of the following manners: (i) by a given initial distribution $c_k(0) = M \delta_{k1}$ (here $Q = 0$); (ii) by a steady source

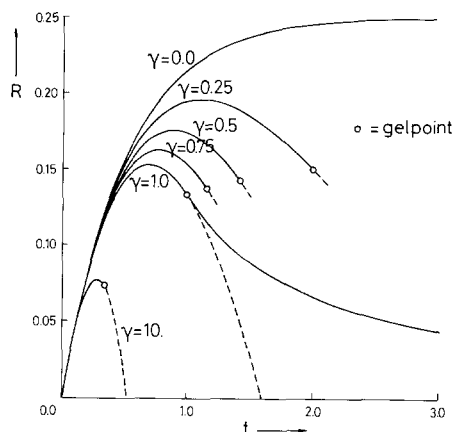


FIG. 3. Cluster concentration $R(t)$ versus time in condensation model B with addition rate constants $K_{ij} = j$ for different values of the parameter γ in the condensation rate constant $K_{ij} = ij\gamma$ ($i, j > 1$) ($\gamma = 0$ yields addition model B). The gel point (where the second moment $\sum k^2 c_k(t)$ diverges) is indicated by an open circle. The solid curves for t below the gel point t_c are the pre-gelation curves (Eq. [2.23]). The broken lines represent the analytic continuation of the pre-gel results across the gel point. Only for $\gamma = 1$ (corresponding to Flory's model RA_∞) the post-gelation curve (solid line for $t > t_c$) is known through Eq. [2.22].

$Q_k = Q \delta_{k1}$, switched on at $t = 0$ (here $c_k(0) = 0$); (iii) by an infinite reservoir, such that $c_1(t)$ remains constant (here $c_k(0) = c_1 \delta_{k1}$).

It is further convenient to work in non-dimensional variables. In case (i) we rescale the concentrations as $c_k(t) = M \bar{c}_k(\bar{t})$, and the time as $t = \bar{t}/SM$, so that $\sum k \bar{c}_k(\bar{t}) = 1$. In case (ii) we insert $c_k(t) = c_0 \bar{c}_k(\bar{t})$ and $t = t_0 \bar{t}$ into [2.24] and choose c_0 and t_0 such that the source strength Q and the constant S are equal to unity in the rescaled equation. The result is $c_0 = (Q/S)^{1/2}$ and $t_0 = (QS)^{-1/2}$. In case (iii) we rescale $c_k(t) = c_1 \bar{c}_k(\bar{t})$ and $t = \bar{t}/Sc_1$, such that monomer concentration and constant S are unity in the rescaled equation.

Henceforward we only work with non-dimensional variables, we drop the bar on \bar{c}_k and \bar{t} , and use the kinetic equation [2.24] with $M = 1$ in (i); $Q = 1$ in (ii); $c_1 = 1$ in (iii); and $S = 1$ in all cases.

As a preparation for the solution of these models in the following sections, it is con-

venient to introduce a new "time" variable τ , defined as

$$d\tau = c_1(t)dt$$

or

$$t = \int_0^\tau d\tau' (C_1(\tau'))^{-1}, \quad [2.25]$$

and to consider the size distribution as a function of τ , i.e.,

$$c_k(t) \equiv C_k(\tau). \quad [2.26]$$

In terms of the new time variable τ the non-linear kinetic equations for $k \geq 2$ reduce to a set of coupled linear relaxation equations for $C_k(\tau)$ with a time dependent "source" $Q_k = s_1 C_1(\tau) \delta_{k2}$. This set of equations can be solved most conveniently by introducing generating functions:

$$f(x, \tau) = \sum_{k=2}^\infty s_k C_k(\tau) e^{kx}$$

$$g(x, \tau) = \sum_{k=2}^\infty C_k(\tau) e^{kx}. \quad [2.27]$$

After these preparations we can transform [2.24] into

$$dC_1(\tau)/d\tau = -2s_1 C_1(\tau) - f(0, \tau) + Q \quad [2.28]$$

$$\partial g(x, \tau) / \partial \tau$$

$$= (e^x - 1)f(x, \tau) + s_1 C_1(\tau) e^{2x}, \quad [2.29]$$

where $g(x, \tau)$ satisfies the initial condition $g(x, 0) = 0$, since $C_k(0) = 0$ for $k \geq 2$. If an initial amount of monomers is given, or if the system is coupled to an infinite reservoir, the initial condition on the monomer concentration is $c_k(0) = \delta_{k1}$, whereas $c_k(0) = 0$ in the presence of a source. We consider six different cases:

model A: $s_k = 1 (k \geq 2)$;

$$Q = 0(\text{no source}); c_1(0) = 1$$

model B: $s_k = k (k \geq 2)$;

$$Q = 0(\text{no source}); c_1(0) = 1$$

model C: $s_k = k (k \geq 1)$;

$$Q = 1(\text{source}); c_1(0) = 0$$

model D: $s_k = 1 (k \geq 1)$;

$$Q = 1(\text{source}); c_1(0) = 0$$

model E: $s_k = 1 (k \geq 2)$; $c_1(t) = 1(\text{reservoir})$

model F: $s_k = k (k \geq 2)$; $c_1(t) = 1(\text{reservoir})$

Except in model D, we shall calculate for all these models the time dependence of the size distribution and its first few moments $M_n(t) \equiv \mu_n(\tau)$, defined as

$$M_n(t) = \mu_n(\tau) = \sum_{k=1}^\infty k^n c_k, \quad [2.30]$$

where $\mu_n(\tau)$ is considered as a function of τ . The moment $M_0(t)$ denotes the total number of clusters in the system, and $M_1(t) = M(t)$ is the total mass. A possible measure for the cluster size is given by the number average of polymerization:

$$U(t) = M_1(t)/M_0(t). \quad [2.31]$$

For model D only certain properties of the solution, such as the large k -behavior, can be obtained.

3. ADDITION MODELS WITH INITIAL MONOMER SUPPLY

Model A: $K_{11} = 2a$; $K_{1k} = s_k = 1 (k > 1)$,
No Sources

In the present case the two generating functions in [2.27] are equal, and we have chosen $s_1 = a$ in [2.28]–[2.29]. The solution of the differential equation [2.29], satisfying $g(x, 0) = 0$, reads:

$$g(x, \tau) = a e^{2x} \int_0^\tau d\tau' C_1(\tau') \times \exp[(\tau - \tau')(e^x - 1)]. \quad [3.1]$$

The size distribution follows from [2.27] and [3.1] by Taylor expansion:

$$C_k(\tau) = a \int_0^\tau d\tau' C_1(\tau') e^{-\tau+\tau'} \times (\tau - \tau')^{k-2} / (k-2)!. \quad [3.2]$$

It simplifies considerably for large k , where

the dominant contribution comes from a small τ' region around the origin. By putting $\tau' = y/k$ and using the relation $(\tau - \tau')^{k-2} \simeq \tau^{k-2} \times \exp(-y/\tau)$, valid for $k \rightarrow \infty$, we obtain in the large k -limit:

$$C_k(\tau) \simeq a e^{-\tau} \tau^{k-1} / (k-1)! \quad (k \rightarrow \infty). \quad [3.3]$$

To derive this we had to use the fact $C_1(0) = 1$ only. Physically this means that there are no backcoupling effects of the changing $C_k(\tau)$ on the "source" $C_1(\tau)$ present in [3.3], as these effects do not instantaneously propagate to large k -value.

For general k the solution [3.2] depends on the unknown $C_1(\tau)$. Combination of [2.28] with $g(0, \tau)$ in [3.1] yields, after differentiating with respect to τ :

$$\ddot{C}_1 + 2a\dot{C}_1 + aC_1 = 0, \quad [3.4]$$

to be solved with $C_1(0) = 1$ and $\dot{C}_1(0) = -2a$. Dots denote differentiations with respect to τ .

Case $K_{11} = 2(a = 1)$

A simple case occurs for $a = 1$, where the size distribution follows from [3.4] and [3.2] as

$$C_1(\tau) = e^{-\tau}(1 - \tau) \quad [3.5a]$$

$$C_k(\tau) = e^{-\tau} \left\{ \frac{\tau^{k-1}}{(k-1)!} - \frac{\tau^k}{k!} \right\}. \quad [3.5b]$$

The moments [2.30] can be calculated from [3.5]

$$\mu_n(\tau) = e^{-\tau} \left(\frac{d}{d\tau} - 1 \right) \left(\tau \frac{d}{d\tau} \right)^n (e^\tau - 1). \quad [3.6]$$

The first few are explicitly given by

$$\begin{aligned} \mu_0 &= e^{-\tau}, & \mu_1 &= 1; & \mu_2 &= 2\tau + 1; \\ \mu_3 &= 3\tau^2 + 6\tau + 1. \end{aligned} \quad [3.7]$$

The original time variable can be recovered from [2.25] and [3.5] as

$$t = e[E_1(1 - \tau) - E_1(1)], \quad [3.8]$$

where $E_1(\tau)$ is an exponential integral (24).

The equations [3.5]–[3.8] represent the exact solution of this addition model in para-

metric form. The parameter τ can be eliminated in the limiting cases of small and large times. Only the latter will be given explicitly. For $t \simeq 0$ we find $\tau \simeq t - t^2 + \dots$, and for $t \rightarrow \infty$:

$$\tau \simeq 1 - \exp[-\gamma - E_1(1) - t/e], \quad [3.9]$$

where γ is Euler's constant. As $\tau \rightarrow \tau_\infty = 1$ or $t \rightarrow \infty$ the supply of monomeric units, $c_1(t)$, is exhausted and addition reactions stop. The size distribution $c_k(t)$ and its moments $M_n(t)$ approach a finite limiting value, $C_1(\tau_\infty)$ and $\mu_n(\tau_\infty)$, exponentially fast:

$$c_1(t) \simeq \exp[-1 - \gamma - E_1(t) - t/e] + \dots$$

$$c_k(t) \simeq (k-1)/ek! - c_1(t)(k^2 - 3k + 1)/k! + \dots$$

$$M_0(t) \simeq 1/e + c_1(t) + \dots$$

$$M_2(t) \simeq 3 - 2ec_1(t) + \dots \quad [3.10]$$

For this version of model A with $K_{11} = 2(a = 1)$ Samsel and Perelson (4) have already obtained the results [3.5a] and [3.8] with τ replaced with $\tau = \log U$ (where $U = 1/M_0$ is the average cluster size). Here we have, in addition, determined the complete size distribution and all its moments.

Case $K_{11} = 2a$

For general values of a one obtains from [3.4] and [3.3] for $a > 1$ after some algebra:

$$\begin{aligned} C_1(\tau) &= [e^{-\tau}/2(a-1)] \{-p_1 e^{-p_1 \tau} + (1 \rightarrow 2)\} \\ &= e^{-a\tau} [\cosh b\tau - (a/b) \sinh b\tau] \\ C_k(\tau) &= [a e^{-\tau}/2(a-1)] p_1^{2-k} \\ &\quad \times \left\{ \sum_{l=0}^{k-2} (p_1 \tau)^l / l! - e^{p_1 \tau} \right\} + (1 \rightarrow 2). \end{aligned} \quad [3.11]$$

Here $(1 \rightarrow 2)$ indicates that a similar term with p_1 replaced by p_2 should be added, where

$$p_{1,2} = 1 - a \pm b; \quad b = [a(a-1)]^{1/2}. \quad [3.12]$$

The most convenient way to calculate the lower moments is not from the generating function [3.1], but directly from [2.28]. This yields

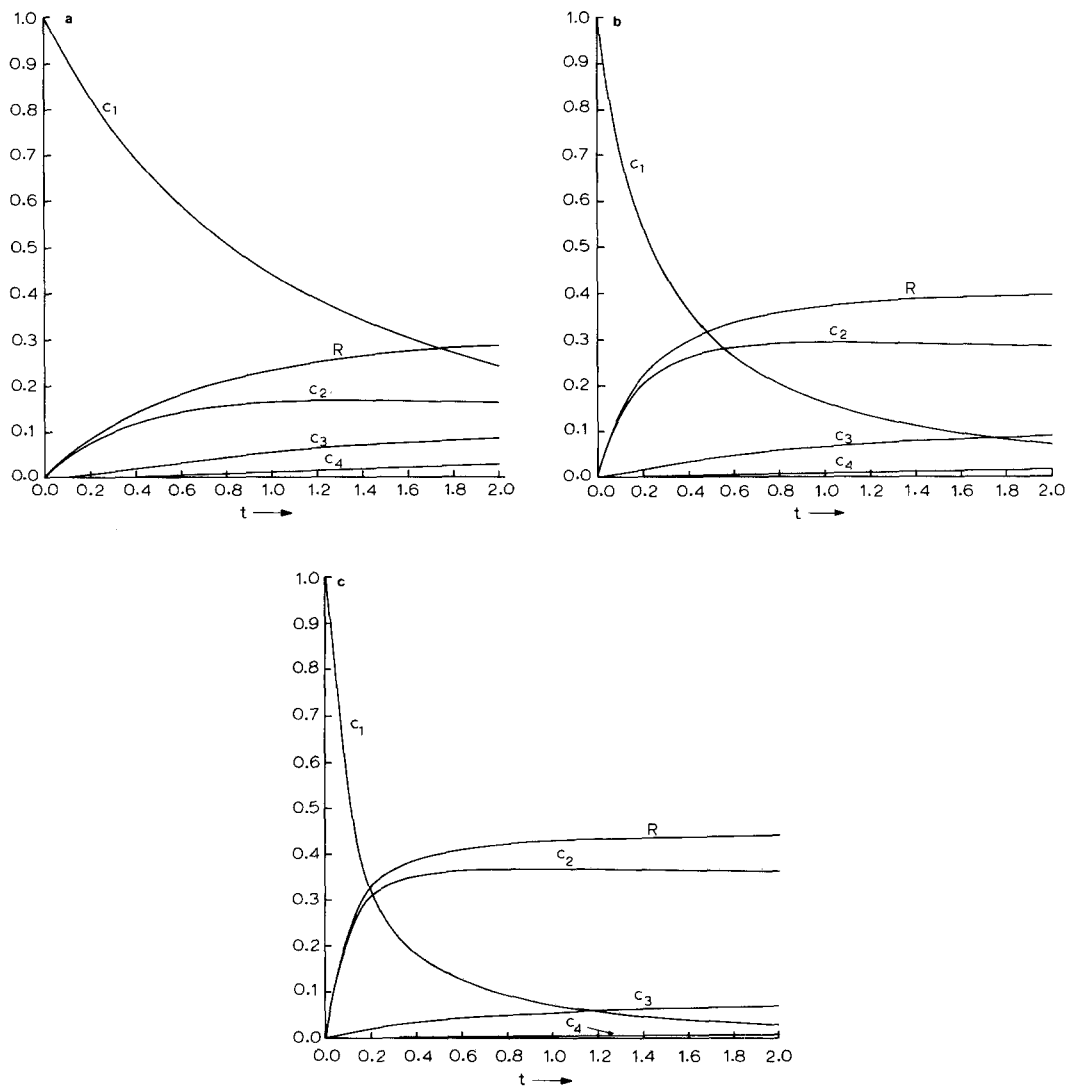


FIG. 4. Size distribution $c_k(t)$ ($k = 1, 2, 3, 4$) and cluster concentration $R(t)$ versus time for addition model A with initial condition $c_k(0) = \delta_{k1}$ and rate constants $K_{1j} = 1$ ($j > 1$) for different choices of monomer-monomer rate constants: (a) $K_{11} = 1$; (b) $K_{11} = 4$; and (c) $K_{11} = 10$ (see also Figs. 2a and b for $\gamma = 0$). Note the dependence of $R(t)$ and $c_2(t)$ on K_{11} ; for larger K_{11} values more clusters are formed which are smaller on the average.

$$\begin{aligned}
 M_0(t) &= \mu_0(\tau) = (1 - 2a)c_1 - \dot{c}_1 \\
 &= e^{-a\tau} \cosh b\tau.
 \end{aligned}
 \tag{3.13}$$

$$\begin{aligned}
 M_2(t) &= \mu_2(\tau) \\
 &= M_2(0) + 2\tau + 2(a - 1) \\
 &\quad \times \int_0^\tau d\tau' C_1(\tau') = 1 + 2\tau \\
 &\quad + 2(b/a)e^{-a\tau} \sinh b\tau.
 \end{aligned}
 \tag{3.14}$$

The total mass, $M_1 = 1$, is conserved and M_2 is obtained by integrating the moment equation; i.e.,

In the limit $a \rightarrow 1$ we recover the results for $K_{11} = 2$. The relation between t and τ follows from [2.25] and [3.11] as

$$t = \int_0^\tau ds e^{as} \times [\cosh bs - (a/b) \sinh bs]^{-1}, \quad [3.15]$$

but the integral does not reduce to any special function. It has been evaluated numerically to determine the size distribution $c_k(t)$ and the number of clusters $R(t) = \sum_{k=2}^\infty c_k(t)$ for different values of $K_{11} = 2a$, as shown in Fig. 4. The same results are also contained in Figs. 1 and 2 with $\gamma = 0$. For $t \rightarrow 0$ one finds $\tau \simeq t$, and for $t \rightarrow \infty$ one finds $\tau \rightarrow \tau_\infty$ where τ_∞ is the root of $C_1(\tau) = 0$. The approach to the limiting value is described by $\tau_\infty - \tau \simeq (\exp(-\omega t))$, as $t \rightarrow \infty$, where $\omega = \sqrt{a} \times \exp(-a\tau_\infty)$. Therefore the concentration of monomers decays exponentially: $c_1 \sim \exp(-\omega t)$ and c_k and M_n approach their limiting values. $C_k(\tau_\infty)$ and $\mu_n(\tau_\infty)$, respectively, at an exponential rate. For $a < 1$ the derivation proceeds along similar lines. The difference is that hyperbolic functions are replaced by trigonometric ones. Of special interest is the case $a = 1/2$, where all rate constants are equal, i.e., $K_{ij} = K_{11} = 2a = 1$. The size distribution becomes:

$$C_1(\tau) = \sqrt{2} e^{-\tau/2} \cos(\tau/2 + \pi/4)$$

$$C_k(\tau) = \frac{1}{2} 2^{k/2} e^{-\tau/2} \sin(k\pi/4 - \tau/2) - \frac{1}{2} 2^{k/2} e^{-\tau} \sum_{l=0}^{k-2} \sin[(k-l)\pi/4] \times (\tau/\sqrt{2})^l / l! \quad [3.16]$$

and the first few moments are:

$$M_0(t) = \mu_0(\tau) = e^{-\tau/2} \cos \tau/2$$

$$M_2(t) = \mu_2(\tau) = 1 + 2\tau - 2e^{-\tau/2} \sin \tau/2. \quad [3.17]$$

The integral expression for $t(\tau)$, corresponding to [3.15], has been evaluated numerically.

Model B: $K_{11} = 1 - \beta$ ($\beta < 1$); $K_{jk} = k$ ($k > 1$) No Sources

In this case, where we have put $s_1 = 1/2(1 - \beta)$ in [2.28] and [2.29] the equation for $C_1(\tau)$ does not couple to [2.29], since $f(0, \tau) = 1 - C_1(\tau)$ as a consequence of mass conservation $\sum kC_k = 1$. The equation for C_1 can be solved directly and the solution with $C_1(0) = 1$ reads

$$C_1(\tau) = \frac{1}{\beta} \{1 + (\beta - 1)e^{\beta\tau}\}. \quad [3.18]$$

The original time variable can be recovered from [2.25] and is given by the relation

$$e^{-\beta\tau} = 1 - \beta + \beta e^{-t}. \quad [3.19]$$

As $t \rightarrow 0$ one finds $\tau \simeq t$, and as $t \rightarrow \infty$ one finds: $\tau \simeq \tau_\infty - e^{-t}/(1 - \beta)$, where $\tau_\infty = -\beta^{-1} \times \ln(1 - \beta)$.

The monomer concentration in terms of the original time variable is

$$c_1(t) = [\beta + (1 - \beta)e^t]^{-1}. \quad [3.20]$$

The generating functions [2.27] are related as $f = g_x$, and [2.29] reduces to a partial differential equation, that can be solved by the method of characteristics:

$$\frac{d\tau}{ds} = 1; \quad \frac{dx}{ds} = 1 - e^x;$$

$$\frac{dg}{ds} = \frac{1}{2} (1 - \beta) C_1(\tau) e^{2x}. \quad [3.21]$$

The solution satisfying $g(x, 0) = 0$ becomes

$$g(x, \tau) = \frac{1}{2} (1 - \beta) \int_0^\tau d\tau' C_1(\tau') \times [1 - e^{\tau-\tau'}(1 - e^{-x})]^{-2} \quad [3.22]$$

and the size distribution $C_k(\tau)$ for $k \geq 2$ follows by Taylor expansion:

$$C_k(\tau) = \frac{1}{2} (1 - \beta)(k - 1) \times \int_0^\tau d\tau' C_1(\tau') e^{-2\tau+2\tau'} (1 - e^{-\tau+\tau'})^{k-2}. \quad [3.23]$$

The asymptotic expression for large k sim-

plifies considerably, since the dominant contribution to the τ' integral comes from a small region around $\tau' = 0$, so that $C_1(\tau) \simeq c_1(0) = 1$. By putting $\tau' = y/k$ and using the relation $(1 - e^{-\tau'})^{k-2} \simeq (1 - e^{-\tau})^{k-2} \exp[-y/(e^\tau - 1)]$, valid for large k , we obtain for $k \rightarrow \infty$:

$$C_k(\tau) = \frac{1}{2} (1 - \beta)e^{-\tau}(1 - e^{-\tau})^{k-1}. \quad [3.24]$$

$$\text{Case } K_{11} = 2(\beta = -1)$$

The special case $\beta = -1$ is again simple. With the help of [3.20] and [3.23] one obtains the size distribution for all k :

$$C_k(\tau) = k^{-1}(1 - e^{-\tau})^{k-1}((k + 1)e^{-\tau} - 1)$$

$$c_k(t) = k^{-1}(1 - e^{-t})^{k-1}$$

$$\times (2 - e^{-t})^{-k}(k - 1 + e^{-t}). \quad [3.25]$$

In the last line of [3.25] the variable τ has been eliminated in favor of the original time variable t , using [3.19] for $\beta = -1$; i.e.,

$$e^\tau = 2 - e^{-t}. \quad [3.26]$$

The moments can be calculated directly from [2.30], yielding

$$\mu_0(\tau) = 1 - \tau$$

$$\mu_n(\tau) = \left(\frac{d}{d\tau} - 1\right) \left[(e^\tau - 1) \frac{d}{d\tau} \right]^{n-1} (e^\tau - 1) \quad (n \geq 1). \quad [3.27]$$

The first few read explicitly:

$$\mu_2(\tau) = e^{2\tau}; \quad \mu_3(\tau) = 4e^{3\tau} - 3e^{2\tau}. \quad [3.28]$$

In terms of the original time variable t we have

$$M_0(t) = 1 - \log(2 - e^{-t})$$

$$M_2(t) = (2 - e^{-t})^2$$

$$M_3(t) = (2 - e^{-t})^2(5 - 4e^{-t}). \quad [3.29]$$

$$\text{Case } K_{11} = 1 - \beta \quad (\beta < 1)$$

For arbitrary values of β the size distribution

$C_k(\tau)$ can be calculated from [3.23] and [3.18] by expanding $[\dots]^{k-2}$ in powers of $e^{-\tau+\tau'}$ using Newton's binomial formula. $C_k(\tau)$ is found to be a polynomial of degree k in $e^{-\tau} = [1 - \beta + \beta e^{-t}]^{1/\beta}$. It will not be written here, but may be easily calculated. In the special case $\beta = 0$ (i.e., $K_{11} = 1$) one obtains the relatively simple expression:

$$C_k(\tau) = \frac{1}{2} \left\{ \alpha^{k-1} - \alpha^k + k^{-1} \sum_{l=1}^k \alpha^l / l - \tau / k \right\} \quad (k \geq 2) \quad [3.30]$$

with $\alpha = 1 - e^{-\tau}$ and $\tau = 1 - e^{-t}$ on account of [3.19]. The moments for general β can be calculated from the generating function [3.22], combined with [3.18] and the relation:

$$\mu_n(\tau) = c_1(\tau) + \left[\left(\frac{\partial}{\partial x} \right)^n g(x, \tau) \right]_{x=0}. \quad [3.31]$$

One finds for the first few:

$$\begin{aligned} \mu_0(\tau) &= \frac{1 + \beta^2}{2\beta^2} + \left(\frac{1 - \beta}{2\beta} \right) \tau - \left(\frac{1 - \beta^2}{2\beta^2} \right) e^{\beta\tau} \\ \mu_2(\tau) &= \frac{1 + \beta}{2\beta} + \frac{3}{2} \left(\frac{1 - \beta}{2 - \beta} \right) e^{2\tau} \\ &\quad - \frac{(1 - \beta^2)}{\beta(2 - \beta)} e^{\beta\tau}. \quad [3.32] \end{aligned}$$

The large t -behavior of moments and distribution function can be studied along the lines of the previous sections by expanding $C_k(\tau)$ and $\mu_n(\tau)$ in powers of $\tau_\infty - \tau = e^{-t}/(1 - \beta)$, where τ_∞ is defined below [3.19]. In Fig. 5 the size distribution $c_k(t)$ and number of clusters $R(t) = M_0(t) - c_1(t)$ are plotted versus time for $K_{11} = 1(\beta = 0)$. The same results are contained in Fig. 3 for $\gamma = 0$. For a comparison with the results of model A we refer to Table I. (See also Fig. 3 for $\gamma = 0$.) In models A and B, all moments approach finite values (cf. Figs. 4 and 5). In model A (with $K_{11} = 2$), $M_0(\infty) = 0.37$, $M_2(\infty) = 3$ and in model B (with $K_{11} = 2$), $M_0(\infty) = 1 - \ln 2 \simeq 0.31$, and $M_2(\infty) = 4$. Hence in the latter model the same amount of mass ($M_1 = 1$) is dis-

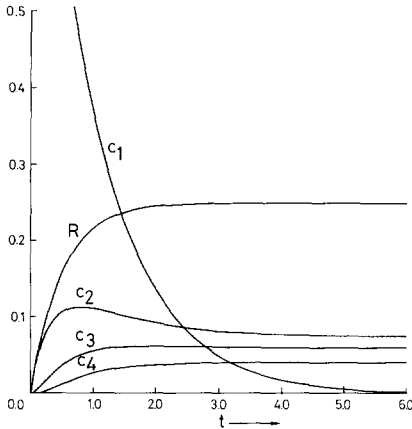


FIG. 5. Size distribution $c_k(t)$ ($k = 1, 2, 3, 4$) and cluster concentration $R(t)$ versus time for addition model B with rate constants $K_{1j} = j$ ($j \geq 1$) and initial condition $c_k(0) = \delta_{k1}$. The concentration $c_k(t)$ of larger cluster sizes k increases faster through faster monomer adsorption and consequently $R(\infty)$ is smaller than in the comparable case of Fig. 4a.

tributed over a smaller total number of clusters, necessarily having a larger average size. This is to be expected physically from the larger coagulation rates.

For both models, if we decrease (increase) the value of K_{11} the value of $M_0(\infty)$ decreases (increases) accordingly. For example, if we put $K_{11} = 1$ in model A we find $M_0(\infty) = 0.32$, where $M_0(\infty) = 0.37$ for $K_{11} = 2$. This is again to be expected. Due to the smaller coagulation

rate for the formation of dimers, more monomers are available to condense onto larger clusters.

4. ADDITION MODELS WITH SOURCES

Some properties of the solution drastically change if the monomeric units are being produced by a steady source, $Q_k = \delta_{k1}$, instead of being present in a finite amount at the initial time. The relevant kinetic equations [2.24] for the choice $s_k = k$ ($k \geq 1$) are

$$dc_1/dt = -c_1M_1 - c_1^2 + 1$$

$$dc_k/dt = (k - 1)c_{k-1}c_1 - kc_kc_1 \quad (k \geq 2), \quad [4.1]$$

to be solved with $c_k(0) = 0$. One easily shows that the total mass of particles $M_1 = \sum kc_k = t$. The differential equation for $c_1(t)$ is a Riccati equation. Its solution with $c_1(0) = 0$ can be obtained straightforwardly through the substitution $c_1 = 1/t + 1/u(t)$. The result is

$$c_1(t) = F(t)/N(t) \quad [4.2]$$

with

$$N(t) = tF(t) + \exp(-1/2t^2)$$

$$F(t) = N'(t) = \int_0^t dx \exp(-1/2x^2), \quad [4.3]$$

where $F(t) = \sqrt{\pi/2} \operatorname{erf}(t/\sqrt{2})$ is related to the error function (24). Its limiting behavior is

TABLE I

Properties of the Solutions for the Various Addition Models with $K_{11} = 2$

Model	$\tau \leftrightarrow t$	$c_k(t), k \rightarrow \infty$	$c_k(t), t \rightarrow \infty$	$t \rightarrow \infty$		
				R	M_1	M_2/M_1
A	$t = e(E_1(1 - \tau) - E_1(1))$	$\frac{e^{-\tau} \tau^{k-1}}{(k-1)!}$	$(k-1)/ek! + \mathcal{O}(e^{-t/k})$	0.37	1	3
B	$e^t = 2 - e^{-t}$	$e^{-\tau}(1 - e^{-\tau})^{k-1}$	$2^{-k}(k-1)/k - \mathcal{O}(e^{-t})$	0.31	1	4
C	$e^t = N(t)$	$\left(\frac{\sqrt{\pi}}{2k}\right)^{1/2} (N-1)^{k-1/4} N^{-k}$	$t^{-1} + \mathcal{O}(t^{-2})$	0.97	t	0.72t
E	$\tau = t$	$\frac{e^{-t} t^{k-1}}{(k-1)!}$	$1 - \mathcal{O}(e^{-t} t^{k-2})$	t	$1/2 t^2$	$1/3 t$
F	$\tau = t$	$e^{-t}(1 - e^{-t})^{k-1}$	$k^{-1} - \mathcal{O}(e^{-t})$	t	$2e^t$	$3/2 e^t$

$$c_1(t) \simeq t^{-1} - (2/\pi)^{1/2} t^{-2} \times \exp(-1/2t^2) + \dots \quad (t \rightarrow \infty)$$

$$\simeq t - 2t^3/3 + \dots \quad (t \rightarrow 0). \quad [4.4]$$

For later use it is convenient to define a new time variable τ through $\tau = \int_0^t dt' c_1(t')$, where $c_1(t)$ in [4.2] is a known function of t , yielding

$$e^\tau = N(t) \simeq t\sqrt{\pi/2} + t^{-2} \exp(-t^2/2) \quad (t \rightarrow \infty)$$

$$\simeq 1 + 1/2t^2 \quad (t \rightarrow 0). \quad [4.5]$$

The kinetic equations [4.1] for c_k with $k \geq 2$ are identical to those in model B, provided we change to the new time variable with $d\tau = c_1(t)dt$. The solution as a function of τ is given by [3.23]. It can be expressed in the original t variable with the help of [4.4] and [4.5]:

$$c_k(t) = [(k - 1)/N^2(t)] \times \int_0^t dt' F^2(t') [1 - N(t')/N(t)]^{k-2}. \quad [4.6]$$

All integrals in [4.6] can be expressed in error functions, but the calculations soon become very laborious. We only quote

$$c_2(t) = \{tF^2(t) + 2F(t) \exp(-t^2/2) - \sqrt{2}F(t\sqrt{2})\}/N^2(t). \quad [4.7]$$

We first study the properties of $c_k(t)$, starting with the *large k-behavior* at fixed t . It can be calculated from [4.6] in much the same way as for models in A and B. The dominant contribution to [4.6] comes from a small region about $t' = 0$, proportional to $1/\sqrt{k}$. By making the substitution $t' = y/\sqrt{k}$ one finds with the help of [4.5] the following equality for large k :

$$[1 - N(t')/N]^{k-2} \simeq [(N - 1)/N]^{k-2} \exp[-y^2/2(N - 1)]. \quad [4.8]$$

This factor cuts off the integration over $y = t/\sqrt{k}$ at a finite value, so that the large k -limit can be taken under the integral sign. The result is

$$c_k(t) \simeq (\pi/2k)^{1/2} (N - 1)^{k-1/2} N^{-k} \quad (k \rightarrow \infty, t \text{ fixed}) \quad [4.9]$$

Qualitatively we have here: $c_k \sim k^{-1/2} \lambda^k$ to be compared with $c_k \sim \lambda^k/(k - 1)!$ in model A and $c_k \sim \lambda^k$ in model B, where λ is some number smaller than unity.

The *short time behavior* of $c_k(t)$ can be deduced from [4.6] with the help of [4.5] and [4.3]:

$$c_k(t) \simeq (k - 1)! t^{2k-1} / (2k - 1)!! \quad (t \rightarrow 0), \quad [4.10]$$

to be compared with $c_k \simeq t^{k-1}/(k - 1)!$ in model A, and $c_k \simeq t^{k-1}$ in model B. The *long time behavior* of $c_k(t)$ can be determined most conveniently from the kinetic equation [4.1]. Using [4.4] and [4.7] one finds

$$c_k(t) \simeq 1/t - 2\pi^{-1/2}(k - 1)/t^2 + \dots \quad (k > 1, t \rightarrow \infty). \quad [4.11]$$

Note that the monomer concentration $c_1(t)$ approaches its asymptotic form, $1/t$, much faster than $c_k(t)$ does (cf. [4.4]).

Next, we study the *moments* $M_n(t)$, which may be obtained from the generating function $g(x, t)$, given by [3.22] (with $\beta = -1$) as a function of τ . Changing to the original time variable with $d\tau = c_1(t)dt$ and using [4.2] and [4.5] yields

$$g(x, t) = \int_0^t dt' F^2(t') \times [N(t') + N(t)(e^{-x} - 1)]^{-2}. \quad [4.12]$$

With the help of [3.31] one derives for the moments:

$$M_0(t) = c_1 + \int_0^t dt' F^2 N^{-2}$$

$$M_1(t) = c_1 + 2N \int_0^t dt' F^2 N^{-3} = t$$

$$M_2(t) = c_1 + 6N^2 \int_0^t dt' F^2 N^{-4} - 2N \int_0^t dt' F^2 N^{-3}. \quad [4.13]$$

The result, $M_1 = t$, can be easily verified by partial integration, using [4.2] and [4.3]. The short time behavior of $M_n(t)$ can be obtained more easily from [2.30], [4.4], and [4.10]:

$$M_n(t) \simeq c_1 + 2^n c_2 \simeq t + t^3(2^n - 2)/3 \quad (t \rightarrow 0) \quad [4.14a]$$

to be compared with

$$M_n(t) \simeq 1 + (2^n - 2)t \quad (t \rightarrow 0) \quad [4.14b]$$

in models A and B.

The long time behavior can be deduced from [4.13], where the integrals $\int F^2 N^{-k}$ with $k \geq 2$ approach a constant value as time goes to infinity. One easily verifies for $t \rightarrow \infty$:

$$M_n(t) \simeq (n + 1)! N^n \int_0^\infty dt' F^2 N^{-n-2} \simeq n! \alpha_n (\pi/2)^{n/2} t^n. \quad [4.15]$$

In the last equality we have used [4.5] and defined

$$\alpha_n = \int_0^\infty dx (N(x))^{-n-1} \exp(-x^2/2), \quad [4.16]$$

where $\alpha_1 = (2/\pi)^{1/2}$, and where $\alpha_0 = 0.969$ and $\alpha_2 = 0.299$ have been calculated numerically. In Fig. 6 we have plotted the size distribution $c_k(t)$ and the number of clusters $R(t) = \sum_{k=2}^\infty c_k(t)$ versus t . The behavior of $c_k(t)$ in model C is very different from that in models A and B, as can be seen by comparing Fig. 6 with Figs. 4 and 5 (see also Fig. 7 where the model A results of Fig. 4 are plotted on the same scale used in Fig. 6). It can also be seen from Table I, comparing the large t -behavior. The approach to the "limiting" distribution is nonuniform. The concentration $c_k(t)$ at fixed k initially increases according to [4.10], it reaches a maximum at a time $t_{\max}(k)$ and then starts to decrease, *disappearing* asymptotically like [4.11] although monomers are being fed into the system at a constant rate. The value of $t_{\max}(k)$ is determined by the condition $dc_k/dt = 0$, which can be solved for large k , using [4.8]. The result is $t_{\max}(k) = 1/2k$. The previous properties can also be formulated differently:

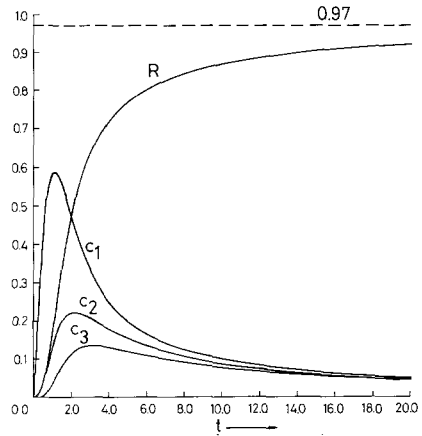


FIG. 6. Size distribution $c_k(t)$ ($k = 1, 2, 3$) and cluster concentration $R(t)$ versus time for addition model C with a monomer source $Q_k = \delta_{k1}$, initial condition $c_k(0) = 0$ and addition rate constants $K_{1j} = j$ ($j \geq 1$). Although monomers are being added at a constant rate the cluster concentration approaches a constant $R(\infty) = 0.97$ and each individual concentration $c_k(t)$ eventually decreases, approaching the limiting curve $y = 1/t$ (see Eq. [4.11]). Note that $c_k = 1/t$ is a solution of Eq. [4.1] with $M_1(t) = t$.

at a given time t , sufficiently large, $c_{k_0}(t)$ with $k_0 = 2t$ has reached its maximum value. For all $c_k(t)$ with $k \geq k_0$ the time dependence is given by [4.10] and for all $c_k(t)$ with $k \leq k_0$ is given by [4.11]. All moments grow like $M_n \propto t^n$ as $t \rightarrow \infty$, whereas they were bounded in models A and B. Remarkably enough the number of clusters $R(t)$ approaches a finite value $\alpha_0 = 0.969$, although the mass in the system keeps increasing linearly with time.

Model D: $K_{1k} = 1 (k > 1)$ with Monomer Source

In the presence of a monomer source formulas [3.1] and [3.2] remain valid. The corresponding equation for $c_1(t) \equiv x(\tau)$ is the equation of motion for a damped, harmonic oscillator $\ddot{x} + (2 + x^{-2})\dot{x} + x = 0$, with boundary conditions $\dot{x}(0) = 1$. We have not been able to find the solution for all times, which is required to determine the relation between t and τ . Still, some properties of the size distribution can be found, e.g., the large k -behavior at fixed t ,

$$c_k \propto \left(\frac{\pi}{2}\right) \frac{\tau^{k-1/2} e^{-\tau}}{(k-1)!},$$

in which, however, τ is an unknown function of time.

5. ADDITION MODELS WITH INFINITE RESERVOIRS

Model E: $K_{11} = 2a; K_{1k} = 1 (k > 1)$

We imagine the system coupled to an infinite reservoir which can emit monomers, in such a manner that $c_1(t)$ remains constant. The transition rate for the reaction $a_k + a_1 \rightarrow a_{k+1}$ is assumed to be independent of the size of the reacting clusters, i.e., $K_{1k} = 1$ for $k > 1$. Then we can use [3.2] with $c_1(t) = 1$, to calculate the resulting size distribution (note the relation $t = \tau$ in this case):

$$c_k(t) = a \int_0^t dt' e^{-t'} (t')^{k-2} / (k-2)! = a e^{-t} \sum_{l=k-1}^{\infty} \frac{t^l}{l!} \quad [5.1]$$

The limit distribution $c_k(\infty) = a$, which is the stationary solution of [2.24] with $s_1 = a$ and $s_k = 1 (k > 1)$, is approached nonuniformly. In fact, we have the limiting behavior:

$$c_k(t) = a \left[1 - e^{-t} \sum_{l=0}^{k-2} \frac{t^l}{l!} \right] = a - \mathcal{O}(e^{-t} t^{k-2}) \quad (t \rightarrow \infty, k \text{ fixed}) \quad [5.2]$$

$$c_k(t) \simeq a \frac{e^{-t} t^{k-1}}{(k-1)!} \quad (k \rightarrow \infty, t \text{ fixed}). \quad [5.3]$$

The latter also represents the short time behavior of c_k . From [5.1] lower moments can be calculated straightforwardly. The first three are given by

$$\begin{aligned} M_0(t) &= 1 + at \\ M_1(t) &= 1 + a(2t + t^2/2) \\ M_2(t) &= 1 + a(4t + 5t^2/2 + t^3/3). \end{aligned} \quad [5.4]$$

The n th moment is a polynomial of degree $n + 1$ in the variable t , and the average cluster size [2.31] grows linearly with $t (t \rightarrow \infty)$.

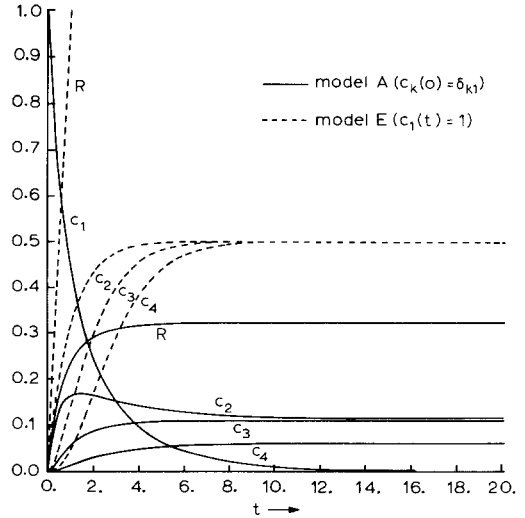


FIG. 7. Size distribution $c_k(t) (k = 1, 2, 3, 4)$ and total cluster concentration $R(t)$ versus time for addition models A and E with rate constants $K_{11} = K_{1j} = 1 (j \geq 1)$ for two types of boundary conditions: model A (full curves) with an initial concentration of one monomer per unit volume and model E (broken curves) with a monomer reservoir keeping $c_1(t) = 1$. Note the nonuniform approach in model E of each $c_k(t) (k > 1)$ to its stationary value $c_k(\infty) = 1/2$, whereas their sum $R(t) = 1/2t$ increases linearly with time (see Table I for a detailed comparison of models A and E).

$$U(t) \simeq 1/2t \quad (t \rightarrow \infty). \quad [5.5]$$

For the special case $K_{11}(a = 1/2)$ the size distribution $c_k(t)$ and number of clusters $R(t) = M_0(t) - 1 = 1/2t$ are plotted versus t in Fig. 7. Although model A and F have the same transition rates ($K_{11} = 2; K_{1k} = 1$) they have different limiting distributions as $t \rightarrow \infty$.

The reason behind this is that in model A only a finite amount of monomers is present, which is used up within a finite time, i.e., in [2.24], $c_1(t) \rightarrow 0$, so that $dc_1/dt \rightarrow 0$. In model E, on the other hand, $c_1(t)$ is kept constant and the limiting distribution is the stationary solution of [2.24] determined by the condition $s_k c_k = s_{k-1} c_{k-1}$. For a further comparison of the different models we refer to Table I.

Model F: $K_{11} = 2a; K_{1k} = k (k > 1)$

Consider again a system coupled to an infinite reservoir of monomers, such that $c_1(t)$

is kept constant, whereas the rate coefficient for the reaction $a_k + a_1 \rightarrow a_{k+1}$ is proportional to the size of the k -cluster, i.e., $K_{1k} = k$. We may use [3.23] with $t = \tau$ to calculate the size distribution at all times:

$$c_k(t) = a(k-1) \int_0^t dt' e^{-2t'} (1 - e^{-t'})^{k-2} \\ = a(1 - e^{-t})^{k-1} (1 + (k-1)e^{-t})/k. \quad [5.6]$$

The limiting distribution $c_k(\infty) = a/k$, which is the stationary solution of [2.24] with $s_1 = a$ and $s_k = k$, is approached nonuniformly:

$$c_k(t) \simeq a(1 - 1/2k (k-1)e^{-t})/k \\ (t \rightarrow \infty, k \text{ fixed}). \quad [5.7]$$

In the coupled limit $k \rightarrow \infty$, $t \rightarrow \infty$, ke^{-t} fixed, the mass distribution kc_k is exponential:

$$kc_k \simeq a(1 + ke^{-t}) \exp(-ke^{-t}). \quad [5.8]$$

We note that in both models E and F the limiting distribution can be found directly from the kinetic Eq. [2.24] by setting all time derivatives equal to zero. Calculating the lower moments from [5.6] is again straightforward. We find

$$M_0 = 1 + at \\ M_1 = 1 + 2a(e^t - 1) \\ M_2 = 1 + a(3e^{2t} - 2e^t - 1). \quad [5.9]$$

From the second of these equations we see that the rate at which monomers are supplied by the infinite reservoir increases exponentially with time. For large t the average cluster size [2.31] grows exponentially fast (cf. [5.5]):

$$U(t) \simeq 2e^t/t \quad (t \rightarrow \infty). \quad [5.10]$$

In Fig. 8 the size distribution $c_k(t)$ ($k > 1$) and number of clusters $R(t)$ are plotted versus time for the special case $K_{1k} = k$ ($a = 1/2$).

In models E and F where monomers are supplied by an infinite reservoir the number of clusters increases linearly with time, but in the latter model the average cluster size grows exponentially with time, while in the former one it only grows as t . We note a similar large

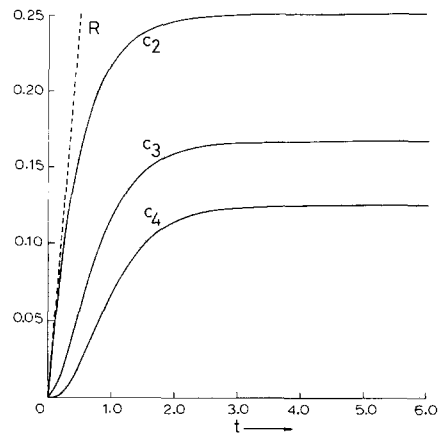


FIG. 8. Size distribution $c_k(t)$ ($k = 2, 3, 4$) and total cluster concentration $R(t)$ for addition model F with rate constants $K_{1j} = j$ ($j \geq 1$) and with a monomer reservoir keeping $c_1(t) = 1$. The stationary size distribution $c_k(\infty) = (2k)^{-1}$ is approached in a nonuniform way, such that the total cluster concentration $R(t) = 1/2t$ increases linearly in time (compare with model E in Fig. 7; see also Table I for a comparison with other addition models).

k -behavior in models E and F, and A and B, respectively. The only difference is due to the different relations between τ and t . In models A and B, τ approaches a finite value τ_∞ , as $t \rightarrow \infty$ and in models E and F we have simply $\tau = t$. These properties have been summarized in Table I.

6. DISCUSSION

Using Smoluchowski's equation we have studied the kinetics of clustering through addition ($a_k + a_1 \rightarrow a_{k+1}$) and through condensation ($a_k + a_l \rightarrow a_{k+l}$; $k, l > 1$). The rate constants K_{ij} for clustering reactions depend on the cluster sizes and vary for different models. We have found a great variety of new analytical results, which provide new insights into the properties of the coagulation equation, and checks on numerical calculations for more complicated models.

The addition and condensation models are special limiting cases (flat disks and needles) of a model, introduced by Samsel and Perelson for coagulation cylinders; their caps are uni-

formly covered with reactive A-groups, their walls with reactive B-groups. A-A bonds lead to linear chain segments, A-B bonds lead to branching.

In the model of flat disks (condensation model A) the rate constants are $K_{11} = \epsilon$, $K_{1j} = 1$ ($j > 1$), and $K_{ij} = \gamma$ ($i, j > 1$), reducing to those of Flory's model RA₂ in the special case $\epsilon = \gamma = 1$. In the needle model one has $K_{11} = 4\epsilon$, $K_{1j} = 3j + 1$ ($j > 1$), and $K_{ij} = (2ij + i + j)\gamma$ ($i, j > 1$), reducing to those of Flory's model A₂RB_∞ for the special case $\epsilon = \gamma = 1$. In the closely related condensation model B the rate constants are $K_{11} = \epsilon$, $K_{1j} = j$ ($j > 1$), and $K_{ij} = ij\gamma$ ($i, j > 1$), reducing to Flory's model RA_∞ for $\epsilon = \gamma = 1$. The last two models exhibit a gelation transition; the first one does not. For the Flory models RA_∞ and A₂RB_∞ the size distribution $c_k(t)$ and its first few moments $M_n(t)$ ($n = 0, 1, 2$) in pre- and post-gelation stage have been given in analytical form in [2.11]–[2.18] and [2.21]–[2.22] for both irreversible and reversible coagulation reactions. Inclusion of fragmentation reactions changes the time dependence of the extent of reaction $\alpha(t)$, but does not affect the functional dependence of $c_k(\alpha)$ and $M_n(\alpha)$ on α . In the RA_∞ model $\alpha(t) = t$ without fragmentation, and $\alpha(t) = \lambda^{-1}(1 - \exp(-\lambda t))$ with fragmentation. In the A₂RB_∞ model $\alpha(t) = 1 - e^{-t}$ without fragmentation and $\alpha(t) = (1 + \lambda)^{-1}\{1 - \exp[-(1 + \lambda)t]\}$ with fragmentation.

The parameter γ in the condensation rate constant K_{ij} ($i, j > 1$) can be used to model an inhibition or stimulation mechanism that lowers ($\gamma < 1$) or raises ($\gamma > 1$) the reactivity of functional groups on clusters as compared to those on monomers. For $\gamma = 0$ the condensation models reduce to pure addition models. The parameter ϵ in the monomer-monomer rate constant $K_{11} = \epsilon$ simulates a similar mechanism. For general values of the parameters (ϵ, γ) in the condensation models A and B we were able to find the monomer concentration $c_1(t)$ and total cluster concentration $R(t) = \sum_{k=2}^{\infty} c_k(t)$ as a function of time with initial condition $c_k(0) = \delta_{k1}$ (see [2.2]–

[2.9] and [2.23] and Figs. 1, 2, 3). In condensation model B (Fig. 3) these solutions are only valid up to the gel-point t_c , defined by the relation $M_2(t_c) = \infty$.

In condensation model A the concentration of monomers $c_1(t)$ depends only weakly on the parameter γ (see Fig. 1), whereas in condensation model B $c_1(t)$ in [2.23] is independent of γ .

In the kinetic equation [2.2] for condensation model A one may neglect terms proportional to γ for sufficiently short times ($t < t_0(\gamma)$), yielding the rate equations for addition model A. The time $t_0(\gamma)$ is determined by the requirement $c_1 \simeq \gamma R$ (see [2.2]), and can be found from the graphs in Fig. 2. E.g. for $\gamma = 1$ we find $t_0(2) \simeq 2.2$ and for $\gamma = 0.5$ we find $t_0(0.5) \simeq 2.8$ in properly normalized time units. In condensation model B the corresponding criterion for neglecting condensation terms is $c_1 \geq \gamma \sum_{k=2}^{\infty} kc_k = \gamma(1 - c_1)$ where mass conservation (in the sol phase) has been used, yielding $t \leq t_0(\gamma) = \ln(1 + 1/\epsilon\gamma)$. The time $t_0(\gamma)$ in condensation model B is smaller than $t_0(\gamma)$ in model A on account of the larger condensation rate constants $K_{ij} = ij\gamma$. These criteria only make sense for small cluster sizes, as can be clearly seen from the values of $t_0(\gamma)$ in condensation model B. For $\gamma \geq 0.75$ the time $t_0(\gamma)$ is already larger than the corresponding gel-point t_c (see Fig. 3), where the infinite cluster appears. In addition model B no gelation occurs.

In Sections 3 to 5 we have studied the corresponding addition models (condensation models with $\gamma = 0$). In model A, D, and E the monomer-cluster rate constant $K_{1k} = 1$ ($k > 1$) and in models B, C, and F, $K_{1k} = k$ ($k > 1$). Both models have been solved for different boundary conditions. In Section 3 we have determined the size distribution $c_k(t)$ and its moments for model A and B, where at the initial time only monomers are present, i.e., $c_k(0) = \delta_{k1}$. In Section 4 with models C and D monomers are supplied by a steady source $Q_k = \delta_{k1}$ and $c_k(0) = 0$. Here only model C with $K_{11} = 2$ has been solved completely. In Section 5 the size distribution $c_k(t)$ and its

moments $M_n(t)$ have been calculated for models E and F, where the system is coupled to an infinite reservoir of monomers that keeps $c_k(t) = 1$.

The effects of boundary conditions in the models A and E with $K_{1k} = 1$ can be clearly seen in Fig. 7, and in the models B, C, and F with $K_{1k} = k$ in Figs. 5, 6, and 8. The time evolution of $c_k(t)$ and $M_n(t)$ strongly depends on the boundary conditions, even for relatively short time. In Table I we have compared the size distribution and its moments for all addition models. Physically, the large time behavior of addition models is not so important, as they should be replaced by condensation models, and also fragmentation terms should be included (16–20).

The approach to equilibrium is in all cases nonuniform in k , which is a general property of solutions of Smoluchowski's equation.

From Table I one sees that at a fixed time t the large k -behavior of the size distribution is the same for the different boundary conditions (compare models A and E and B and F), provided the parameters τ in models A and B is replaced by t in models E and F. (This involves a transformation of the time variable only.)

Our analytical results for the condensation model A (flat disks) and addition model A have been obtained numerically by Samsel and Perelson for different values of the rate constants $K_{11} = \epsilon$ and $K_{ij} = \gamma$ ($i, j > 1$). These authors have also numerically studied the inclusion of break-up terms in the coagulation equation (19). An extensive discussion of the numerical effects of changing the different parameters can be found in Samsel and Perelson's work.

ACKNOWLEDGMENTS

We acknowledge N. G. Van Kampen's help and suggestions in solving some of our differential equations.

REFERENCES

1. Drake, R. L., in "Topics in Current Aerosol Research" (G. M. Hidy and J. R. Brock, Eds.), Vol. 3, Part 2. Pergamon Press, New York, 1972.
2. Cohen, R. J., and Benedek, G. B., *J. Phys. Chem.* **86**, 3696 (1982).
3. Medalia, A. I., in "Surface and Colloid Science" (E. Matijevic, Ed.), Vol. 4, p. 68. Wiley-Interscience, New York, 1971.
4. Samsel, R. W., and Perelson, A. S., *Biophys. J.* **37**, 493 (1982).
5. van Kampen, N. G., "Stochastic Processes in Physics and Chemistry." North-Holland, Amsterdam, 1981.
6. Brock, J. R., *J. Colloid Sci.* **39**, 32 (1972).
7. Ramabhadran, T. E., Peterson, T. W., and Seinfeld, J. H., *AIChE J.* **22**, 840 (1976).
8. Gelbard, F., and Seinfeld, J. H., *J. Colloid Interface Sci.* **68**, 173, 363 (1979).
9. Srivastava, R. C., and Passarelli, R. E., *J. Atmos. Sci.* **37**, 612 (1980).
10. Simons, S., *Phys. Lett. A* **91**, 260 (1982).
11. Heilmann, O. J., "Advances in Molecular Relaxation Processes," Vol. 8, p. 155. Elsevier, Amsterdam, 1976.
12. Stockmayer, W. H., *J. Chem. Phys.* **11**, 45 (1943).
13. Ziff, R. M., *J. Stat. Phys.* **23**, 241 (1980); Ziff, R. M., and Stell, G. E., *J. Chem. Phys.* **73**, 3492 (1980).
14. Leyvraz, F., and Tschudi, H. R., *J. Phys. A. Math. Gen.* **14**, 3389 (1981); **15**, 1951 (1982).
15. Laidler, K. J., "Chemical Kinetics," pp. 50–54. McGraw-Hill, New York, 1965.
16. Blatz, P. J., and Tobolsky, A. V., *J. Chem. Phys.* **49**, 77 (1945).
17. Aizenman, M., and Bak, T. A., *Commun. Math. Phys.* **65**, 203 (1979).
18. Barrow, J. D., *J. Phys. A Math. Gen.* **14**, 729 (1981).
19. Samsel, R. W., and Perelson, A. S., *Biophys. J.*, in press.
20. Van Dongen, P. G. J., and Ernst, M. H., *J. Phys. A. Math. Gen.* **16**, L327 (1983).
21. Flory, P. J., "Principles of Polymer Chemistry," Chap. 9. Cornell University, Ithaca, 1953.
22. Ziff, R. M., Hendriks, E. M., and Ernst, M. H., *J. Stat. Phys.* **31**, 519 (1983).
23. White, W., *Amer. Math. Soc.* **80**, 273 (1980).
24. Abramowitz, M., and Stegun, I. A., "Handbook of Mathematical Functions." Dover, New York.